GROWTH, DISLOCATIONS, AND EXTINCTION OF COBALT WHISKERS

by

BILLY HUGH BAILEY

B. S., Kansas State University, 1961

A MASTER'S THESIS

submitted in partial fulfillment of the

requirements for the degree

MASTER OF SCIENCE

Department of Physics

KANSAS STATE UNIVERSITY
Manhattan, Kansas

1964

Approved by:

R. Dean Dragsdorf
Major Professor

TABLE OF CONTENTS

INTRODUCTION

Growth

Whiskers, filamentary crystals whose diameters are less than 25 μ (6), have been grown by the hydrogen reduction of metal halides (7), (13). This method, outlined by Brenner (7), yields two different mechanisms for growth. Whiskers grown from silver chloride grow at the base, while whiskers grown from copper and iron halides grow at the tip (6). Johnson (13) indicates the whiskers grown from cobalt chloride grow at the tip.

Growth does not occur by the direct condensation of metal vapor but by the adsorption of metal halide molecules on the growing whiskers with further reduction occurring at the tip (7). Brenner (6), quoting Price, Vermilyea, and Webb, states "while the lateral surface may become covered by impurities the tip remains clean because of its rapid advancement." Brenner concludes that impurity adsorption plays an important part in whisker growth.

Brenner has shown that the temperature at the growth site has a pronounced effect on the appearance and size of whiskers. In growing copper whiskers he observed that those grown between 430 and 700°C were straight, between 700 - 850°C were coarse and distorted, and above 850°C were massive particles.

Sears (18) using Cd, Zn, and Ag maintains the critical condition for growth is that the metal halide saturation ratio be kept below a value necessary for two dimensional nucleation (Plate I, fig. 2). The saturation value necessary for two dimensional nucleation is the supersaturation characteristic of the material being deposited (20).

Verma (20) postulates that the low supersaturation ratio that prevails for whisker growth could be a result of the mechanism by which growth occurs.

If growth occurs by means of an axial screw dislocation, (Plate I, fig. 3), there is no need for two dimensional nucleation since a growth step already exists. Whiskers grown from low supersaturations are more regular and well defined (20).

Johnson (13) gives the parameters involved in cobalt whisker growth as the metal halide grain size, the temperature, the water content present during growth, and the hydrogen flow rate.

If growth occurs by means of an axial screw dislocation along the axis of the crystal, the dislocation should be observed using x-ray diffraction techniques as outlined by Bönse (5).

Dislocation

Bönse (5) has shown that if a whisker contains an axial screw dislocation there is a shift in the Bragg angle, the angle for which Bragg's Law $n\lambda = 2d \sin\theta$ produces maximum diffracted x-radiation, throughout the strained region given by

$$\Delta\theta = \delta\theta + \frac{\delta d}{d} \tan\theta \,, \qquad (1)$$

where $\delta\theta$ is the change in Bragg angle due to reorientation of the diffraction planes in the area of strain and δd is the change in lattice spacing of the diffraction planes in the area of strain. If the crystal is set exactly on the diffraction maximum for perfect planes, the change in Bragg angle throughout the strain field produces a decrease in the diffracted intensity from the strained region.

The relation between the change in Bragg angle and the Burgers vector is

$$\Delta\theta = -K \frac{\vec{b} \cdot \vec{n}}{2\pi r} \,. \qquad (2)$$

Here b is the Burgers vector; n is a unit vector normal to the set of diffraction planes; r is the distance from the dislocation line; and K is a term

dependent upon the dislocation type and the direction of incidence of the x-ray beam. For an axial screw dislocation, the condition that $\underline{b} \cdot \underline{n}$ is maximized occurs when the normal to the diffraction planes is parallel to the Burgers vector. This indicates the strain surrounding an axial screw dislocation should be observed with maximum intensity contrast when diffraction occurs from planes perpendicular to the growth axis.

Extinction

Extinction is a result of interference occurring within the crystal between the incident and diffracted x-radiation. Its effect appears as an increase in the normal absorption coefficient. Normal absorption is defined as the diminution of the incident beam traversing a crystal when no diffraction occurs.

James (12) indicates a phase lag of $\frac{\pi}{2}$ radians per reflection for multiple Bragg reflections occurring within a crystal. For twice reflected waves in perfect crystals, the amplitude of the incident wave is reduced by a factor of $e^{-\delta}$ per plane, and the intensity of the incident beam is reduced by $e^{-2\delta}$ per plane. When diffraction occurs in a perfect crystal, this effect is called primary extinction. Primary extinction appears as an increase in the absorption coefficient.

Secondary extinction is defined by means of a crystal made up of small perfect mosaic blocks. The blocks are thin and are misaligned one to another to an extent that maximum reflection does not occur simultaneously from all blocks. Primary extinction does not occur. Secondary reflections occur at the block faces with a phase relationship between the reflected and incident beams which depends on the thickness and orientation of the mosaic blocks. Thus, the reflected beam is not always out of phase with the incident beam and

constructive interference could appear. Secondary extinction is defined as any reduction in the incident beam which results from destructive interference occurring at the block faces. The absorption coefficient associated with secondary extinction appears as a value between the coefficient for perfect crystals and that for normal absorption. The observed or effective absorption coefficient, since the effect of either primary or secondary extinction is an increase in the normal absorption coefficient, may be represented by μ and given by

$$\mu = \mu_o + \mu_o \epsilon = \mu_o (1 + \epsilon) , \tag{3}$$

where μ_o is the normal absorption coefficient and ϵ is the extinction coefficient (14).

The extinction coefficient ϵ has a maximum value for perfect crystals and a minimum $\epsilon = o$ for completely imperfect crystals.

Using equation 3 it is possible to distinguish between primary and secondary extinction. The additional absorption for a perfect crystal is $e^{-2\xi}$ per plane. If t is the thickness per plane of the crystal traversed by the beam then at the Bragg angle

$$t = \frac{d}{\sin \theta} , \tag{4}$$

where d is the interplanar distance, then

$$2\xi = \mu_o \epsilon \frac{d}{\sin \theta} = \frac{\pi N \lambda d e^2}{mc^2 \sin \theta} |f| \tag{5}$$

and

$$\epsilon = \frac{2\xi \sin \theta}{\mu_o d} = \frac{\pi N \lambda e^2}{\mu_o mc^2} |f| , \tag{6}$$

where N represents the number of unit cells per unit volume, λ the characteristic wave length, f the atomic scattering factor, c the speed of light, e the electronic charge on the electron, and m the mass of the electron. The extinction coefficient ϵ represents secondary extinction when $o < \epsilon < \epsilon_p$, where ϵ_p is the primary extinction coefficient given by equation 6. The extinction

coefficient ϵ can be used as a measure of the perfection of the crystal (14).

Johnson (14) outlined a method for measuring the extinction coefficient using a monochromatic beam with diffraction occurring from planes perpendicular to the side of a crystal having a uniformly varying thickness t(y) (Plate IV). Attenuation of the incident beam occurs due to both normal absorption and extinction and results in the effective absorption coefficient given by equation 3. The intensity ratio, for a point on the emulsion due to reflection from a point in the crystal, is

$$\frac{I}{Io} = \frac{\tan\theta}{d} \; t(y) \; \exp\left(\frac{-\mu t(y)}{\cos\theta}\right) . \qquad (7)$$

An extremum occurs when $\frac{dI}{dy} = o$ giving

$$\frac{d}{dy}\left(\frac{I}{Io}\right) = \frac{\tan\theta}{d} \exp\left(\frac{-\mu t(y)}{\cos\theta}\right) \frac{d}{dy}\left(t(y)\right)\left(1 - \frac{\mu t(y)}{\cos\theta}\right) = o$$

or

$$\mu = \frac{\cos\theta}{t(y)} = \mu o \; (1 + \epsilon \;)$$

and

$$\epsilon = \frac{\cos\theta}{t(y)\mu o} - 1 . \qquad (8)$$

The extinction coefficient can be calculated for any crystal when t(y) and the intensity extremum are known.

It was the purpose of this research to determine some of the parameters involved in cobalt whisker growth; to observe the intensity contrast surrounding an axial screw dislocation; and to measure the extinction coefficient of cobalt whiskers.

EXPERIMENTAL PROCEDURE

Growth

Cobalt whiskers were grown by hydrogen reduction of cobalt chloride using the growth procedure given by Brenner (7). An alundum boat filled with the metal halide is placed in a hot furnace through which hydrogen is flowing.

During the period of a few hours, filamentary crystals of the metal grow on the sides of the boat and on the reduced metal in the boat.

The experimental apparatus used for growing whiskers is outlined by Johnson (13). It consisted of a temperature controlled tube furnace, quartz tube, associated equipment necessary to allow a controlled quantity of hydrogen to pass through the tube, and a vacuum system.

Three grams of $CoCl_2 \cdot 6H_2O$, Baker Analyzed Reagent 99.6%, were placed in each boat and three boats were placed in the quartz tube within the furnace. After the tube was sealed from the atmosphere, the vacuum system and furnace were energized. The temperature of the furnace was maintained at 300°C for a period of time sufficient to remove the six waters. After the furnace cooled, the sample ($CoCl_2$) was removed and one gram of $CoCl_2 \cdot 6H_2O$ was added to each boat. The sample was returned to the furnace and temperature adjusted for growth run. Hydrogen flow was started when the furnace temperature was 100°C below that desired for growth and continued until the growth run was complete and the furnace had cooled.

A Rubicon potentiometer and four Chromel-Alumel thermocouples located between the quartz tube and inner furnace wall were used to obtain the furnace temperature profile. Temperature equilibrium existed between furnace and gas within the quartz tube (12). The growth temperature was obtained by relating the position of the boats within the furnace to the furnace temperature profile.

X-Ray Studies

Careful mounting of the whiskers for x-ray diffraction analysis was necessary to minimize the introduction of strain into the whisker. One hundred six whiskers were mounted by attaching the whiskers to the end of

small glass rods with Duco cement. All further handling of the whisker was done indirectly using the glass rod.

Growth axis, crystal multiplicity, geometrical shape, and size were the factors which influenced selection of whiskers for dislocation and extinction studies. All whiskers were mounted with the whisker axis along the axis of a single crystal goniometer. The geometrical shape of the whiskers was obtained by means of an optical goniometer and the size was obtained from photographs taken with a Land Polaroid camera in conjunction with a Leitz microscope. Transmission Laue and rotation x-ray diffraction patterns were taken using a Supper Weissenberg camera and a molybdenum target x-ray tube. From the Laue and rotation patterns the growth axis and crystal multiplicity were determined. This selection process yielded only two whiskers which were satisfactory for dislocation extinction x-ray studies. Both whiskers had a [10·0] growth axis which is perpendicular to the ($\bar{2}$1·0) planes (Appendix 1). From the Laue patterns the twist per unit length of the whisker was determined using the technique of Dragsdorf and Webb (9) and the Burgers vector was calculated using Eshelby's method (11).

A vertical Unicam camera and the condition that diffraction occur from planes perpendicular to the whisker axis required that the whisker be mounted horizontally. This was accomplished by an attachment to the single crystal goniometer. This attachment placed the axis of the whisker perpendicular to the axis of the goniometer. The end of the attachment, to which the whisker was mounted, was made of two pieces coupled in a manner to allow the whisker to be rotated about its own axis. The coupling and the goniometer allowed complete control for positioning the whisker in the incident beam (Plate II, fig. 1, 2, 3).

Utilizing cobalt radiation from a Hilger micro focus unit, Berg-Barrett

(3, 4) topographs were taken of the ($\bar{2}1\cdot0$) planes at various points along the whisker axis. The topographs were magnified and photographed (Plate II) using a Leitz microscope, Land Polaroid camera, and type 46-L small grain projection film with a Leeds and Northrup micro-densitometer. The film was oriented on the densitometer so that scanning occurred perpendicular to the outline of the whisker axis. The density curves were related to the intensity of the diffracted beam producing the curves shown in Plate IV, figures 1, 2.

EXPERIMENTAL RESULTS AND DISCUSSION

Growth

Temperature had a pronounced effect on cobalt whisker growth. The growth versus growth temperature curve (Plate I, fig. 1) shows maximum growth occurred in the range 550 to 600°C and confirms the results obtained by Johnson (13).

Growth occurring at lower temperatures was in the form of whiskers and platelets. The platelets were mostly hexagonal in outline and very thin with uneven surfaces (Plate III, fig. 4). One platelet, estimated at 10 μ thick and 80 μ in maximum cross sectional dimension, revealed a nearly perfect face using reflected light (Plate III, fig. 3). Platelets appeared to grow at temperatures from 400 - 600°C with only whisker growth occurring beyond 600°C.

A mechanism by which platelet growth could occur is that a growth step exists along the line AB (Plate I, fig. 3) rather than along AC as shown. In this manner growth would occur in a plane about a central axis perpendicular to this plane. Since sixfold symmetry appeared with all platelets, this central axis could be the [00$\cdot$1] direction of close-pack hexagonal cobalt. Laue and rotation diffraction patterns yielded no conclusive results for the multiplicity and orientation of the lattice planes of platelets. No further

EXPLANATION OF PLATE I

GROWTH MECHANISMS AND TEMPERATURE DEPENDENCE CURVE

Fig. 1. Bar graph of growth versus growth temperature.

Fig. 2. Two dimensional nucleus on tip of whisker.

Fig. 3. Axial screw dislocation displaying one dimensional nucleation.

PLATE I

FIGURE 1

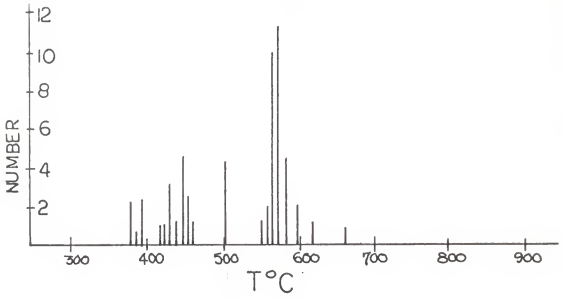

FIGURE 2

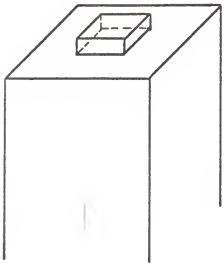

FIGURE 3

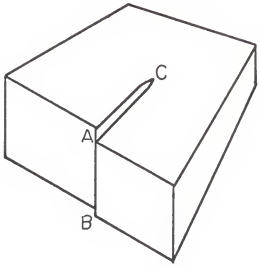

EXPLANATION OF PLATE II

BERG-BARRETT DIFFRACTION TOPOGRAPHS

Fig. 1. Topographs of $(\bar{2}10)$ planes of Co-292 when the horizontal component of the incident radiation was neither parallel nor perpendicular to a whisker face. (Magnification x171)

Fig. 2. Topographs of $(\bar{2}10)$ planes of Co-292 when the horizontal component of the incident radiation was perpendicular to one of the bounding planes. (Magnification 171x)

Fig. 3. Topographs of $(\bar{2}10)$ planes of Co-292 when the horizontal component of the incident radiation was parallel to one of the bounding planes. (Magnification 171x)

PLATE II

FIGURE 1

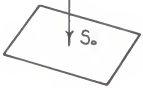

FIGURE 2

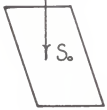

FIGURE 3

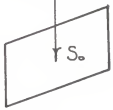

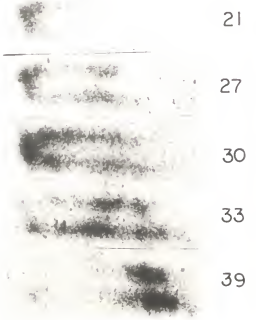

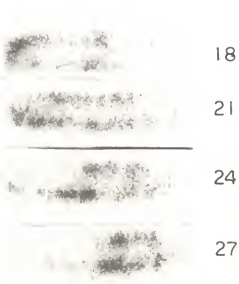

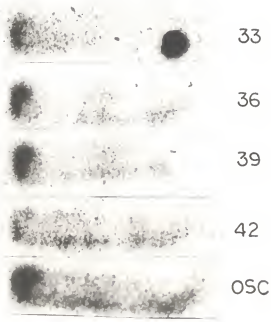

study was conducted on these platelets.

Where large temperature gradients existed, growth occurred in the form of massive crystals with large globules of cobalt adhering to the sides of the boat. Most of the crystals had sharp changes in growth direction, ridges, tapers, and undefinable faces. This agrees with a statement made by Verma (20) that crystals grown where small supersaturations exist are more regular and well defined. For the crystals observed throughout this region, no attempt was made to determine whether growth occurred by two dimensional nucleation or axial screw dislocation.

Difficulty existed in duplication of growth during growth runs. This produced little reliability in the data taken for growth versus hydrogen flow rates. The flow rate was varied from approximately 2 cc to 6 cc per minute in increments of 1 cc per minute with little effect on observed growth. Reduction of the cobalt chloride appeared to be the same in each case although no chemical process was followed to determine the extent of reduction. Little reduction occurred where temperatures were less than 400°C.

X-Ray Analysis

The whiskers will be considered separately and will be identified as Co-292 and Co-206.

Co-292 (Plate III, fig. 2) measured 27x39x500 micron and had (02·1) and (00·2) and their negative planes as bounding faces. Equatorial Laue spots indicated a 15° tilt corresponding to a 0.070 radian per cm lattice twist and a 72 Å Burgers vector.

Using data from the Berg-Barrett topographs (Plate II) and the density curves obtained from the densitometer chart, the diffracted intensity maxima were determined and related to the whisker orientations (Plate IV). The

EXPLANATION OF PLATE III

WHISKERS AND PLATELETS

Fig. 1. Photographs of two faces of Co-206 using reflected light. (x171)

Fig. 2. Photographs of three faces of Co-292 using reflected light. (x171)

Fig. 3. Photograph of platelet with smooth face using reflected light. (x171)

Fig. 4. A. Photograph of platelet using reflected light. (x171)
B. Photograph of side view of platelet.
C. Photograph of platelet using transmitted light.

PLATE III

FIGURE 1

FIGURE 2

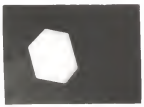

FIGURE 3

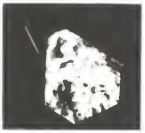

a

b

c

FIGURE 4

EXPLANATION OF PLATE IV

INTENSITY MAXIMA AS RELATED TO WHISKER FACES

Fig. 1. Orientation of diffracted beam intensity maxima with respect to whisker when the horizontal component of the incident beam is neither parallel nor perpendicular to a lateral whisker face.

Fig. 2. Orientation of diffraction beam intensity maxima with respect to whisker when the horizontal component of the incident beam was perpendicular to a lateral whisker face.

PLATE IV

FIGURE 1

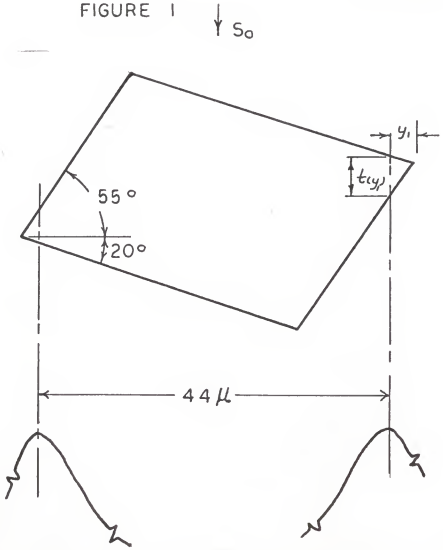

FIGURE 2

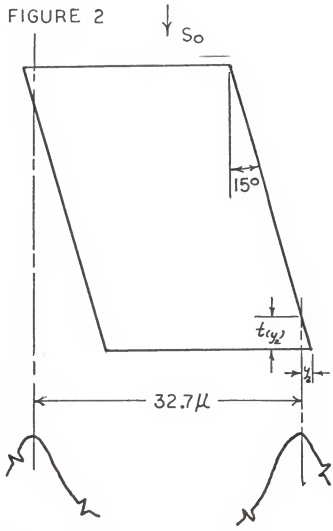

observed intensity maxima indicated that the value of t(y) was similar for both orientations of the whisker shown in Plate IV. From Plate IV

$$t(y_1) = y_1 \ (\text{Tan } 55^\circ + \text{Tan } 20^\circ)$$

$$t(y_1) = 7.3\,\mu$$

and

$$t(y_2) = y_2 \ (\text{Tan } 75^\circ)$$

$$t(y_2) = 8.2\,\mu$$

These similar values of t(y) and the absence of diffracted intensity maxima for the whisker orientation, as shown in Plate II figure 3, indicate the maxima are a result of absorption and extinction rather than the heavy strain region surrounding an axial screw dislocation. Plate II figure 3 shows that absorption was very pronounced and that the diffracted intensity contrast, indicating the heavy strain region, was not observed. As will be shown later, an axial screw dislocation is believed to exist within this whisker and the extinction observed could be an effect of this dislocation. If the intensity maxima were the result of a symmetrical heavy strain region, the distance between maxima would be independent of the orientation of the diffraction planes in the incident beam; whereas, the observed densitometer maxima for the two orientations are separated by $44\,\mu$ (Plate IV, fig. 1) and $32.7\,\mu$ (Plate IV, fig. 2).

The extinction coefficient was calculated assuming there was no axial screw dislocation present in the whisker. This assumption is very nearly correct since the absorption was the dominant factor producing the diffracted intensity maxima. The extinction coefficient, calculated from equation 8, is $\epsilon = 0.64$ when $t(y) = 7.3\,\mu$ (Plate IV, fig. 1) and $\epsilon = 0.46$ when $t(y_2) = 8.2\,\mu$ (Plate IV, fig. 2). The average extinction coefficient is then $\epsilon = 0.55$ and represents secondary extinction. The primary extinction coefficient for cobalt $(\bar{2}1{\cdot}0)$ planes is $\epsilon p = 19$.

A shift along the axis of the whisker between intensity peaks was observed (Plate II, fig. 2, 39') which is due to the divergent beam in conjunction with whisker orientation (Plate V, fig. 1, 2) and twisted diffraction planes resulting from a lattice twist. The lateral shift of the diffraction spots on each side of the whisker axis due to orientation of the crystal in the incident beam is represented by L (Plate V, fig. 1, 2) where

$$L = \frac{7}{\cos \theta} \text{ micron} .$$

The observed angular shift ϕ was 22° (Plate V, fig. 1) measured with respect to a line perpendicular to the whisker axis. The calculated shift due to whisker orientation was 13°. The remaining shift of 9° was assumed to be due to a lattice twist resulting from an axial screw dislocation. The angular tilt of the diffraction planes, with respect to a plane perpendicular to the growth axis, where diffraction occurred, would have to be 3.52×10^{-5} radians to produce an angular shift between the diffraction spots of 9°. This corresponds to a lattice twist of 0.048 radians per cm as compared to the observed value of 0.070 radians per cm obtained from equatorial Laue spots.

The value of the lattice twist calculated from the equatorial spots of the transmission Laue pattern is the value most nearly representing the lattice twist existing within the whisker.

The value of the lattice twist obtained from diffraction planes perpendicular to the axial screw dislocation was calculated from the equation by Eshelby (11)

$$\alpha = \frac{bK}{A} , \qquad (9)$$

where α is the lattice twist, b the Burgers vector, A the cross sectional area of the whisker, and K a term dependent on the ratio of the widths of the two sides of a rectangular whisker. This equation allowed a calculation of the lattice twist only after the magnitude of the Burgers vector was

determined from the topographs and the orientation of the whisker was specified with respect to the incident beam. The magnitude of the Burgers vector is represented by the height of the growth step shown in Plate I, fig. 3.

The height of the growth step and the magnitude of the Burgers vector depend on the radial distance from the screw axis due to the strain introduced into the lattice by the axial screw dislocation. The growth step and the magnitude of the Burgers vector are a maximum at the whisker face where the lattice strain is zero. Thus, only values for the magnitude of the Burgers vector determined where minimum strain exists will yield values, by equation 9, for the lattice twist which are representative of the lattice twist existing within the whisker. The magnitude of the Burgers vector determined from any position along the growth step (Plate I, fig. 3) where strain exists will yield a value for the lattice twist that is smaller than the values for the lattice twist obtained from the surface planes.

The lattice twist was calculated from the topographs and from the orientation of the whisker in the incident beam. The magnitude of the Burgers vector was determined at the positions on the diffraction planes corresponding to the peaks of the diffracted intensity maxima (Plate IV, fig. 1). This value for the magnitude of the Burgers vector was less than the value determined from the transmission Laue pattern. No comparison in the magnitudes between the two values for the lattice twist can be made since the distribution of the strain field within the whisker is not known.

Co-206 (Plate III, fig. 1) is a single crystal which has a geometrical division along the whisker axis caused by growth changes in the bounding faces. The tip measures 7x13x200μ with (00$\cdot$2), (01$\cdot$1), and their negative planes as faces while the base measures 8x9x300μ with (00$\cdot$2), (01$\cdot$1), (0$\bar{1}\cdot$1), (00$\cdot\bar{2}$), and (0$\bar{1}\cdot\bar{1}$) planes as faces. Equatorial Laue spots indicate a 30° tilt

corresponding to a 15.2 Å Burgers vector.

Neither extinction effects nor the diffraction contrast surrounding an axial screw dislocation was observed. The topographs indicated the whisker was irregular in one direction perpendicular to the growth axis. The irregularity appeared as slight bends rather than sharp changes in the growth direction. Throughout these bends there was a strained region resulting in a change in the Bragg angle given by equation 1.

When the regular side of the whisker was perpendicular to the incident x-ray beam the diffraction spot was aligned but broken (Plate VI, figures 1c, 1d). Along the whisker axis there exist sections which were properly oriented for the diffraction which resulted in separate diffraction spots as exemplified in Plate VI, figure 2.

With the irregular side of the whisker perpendicular to the incident beam, the strain regions were observed as a decrease in the diffracted intensity (Plate VI, fig. 1a). The shape of the whisker is shown by the oscillation topograph in Plate VI, figure 1b.

CONCLUSION

Growth

Temperature was shown to have an important influence on the amount of growth which occurred when the Brenner method was used for growing cobalt whiskers. Maximum growth occurred in the temperature range 550 to 600°C.

Platelet growth along with whisker growth resulted when the growth temperatures were less than 600°C. In no case was platelet growth the only growth observed, but those cases where platelet growth did occur also yielded suitable conditions for whisker growth. With these observations it was assumed that platelet growth occurred by a different mechanism than whisker

growth.

The dependence of growth on vapor pressures at the growth site was not determined. Vapor pressure versus temperature data were not available in the temperature regions where growth occurred.

Where large temperature gradients existed, growth was in the form of large coarse crystals which were very irregular.

Although hydrogen had to be present for reduction to occur, variations in the flow rate did not have a major effect on growth.

X-Ray Studies

One hundred six whiskers were examined and only two of these were suitable for x-ray studies. Whisker selection was based on crystal multiplicity, growth axis, size, and shape.

Topographs of the planes perpendicular to the whisker axis were taken of both whiskers. By rotating the whisker about its own axis, topographs of the planes perpendicular to the whisker axis could be taken for any orientation of a whisker face with respect to the incident beam.

The cobalt whisker, Co-206, produced no intensity contrasts within the diffraction maximum for any orientation of a whisker face with respect to the incident beam. Neither the region of heavy strain surrounding an axial screw dislocation nor the effects of extinction were observed.

The other cobalt whisker, Co-292, produced intensity contrast within the diffraction maximum from planes perpendicular to the whisker axis when orientations of the whisker were such that a whisker face was not parallel to the incident beam (Plate II, fig. 1, 2). The intensity contrast within the diffraction maximum was not observed when whisker orientations were such that a whisker face was parallel to the incident beam (Plate II, fig. 3).

The theory by Bönse, neglecting absorption, predicts that a whisker containing an axial screw dislocation and diffraction occurring from lattice planes perpendicular to the whisker axis should produce intensity contrast within the diffraction maximum when the incident beam is parallel to a whisker face.

The absence of intensity contrast within the diffraction maximum, when a whisker face was parallel to the incident beam, indicated either the axial screw dislocation was not present or absorption was so pronounced that the axial screw dislocation was not observed.

A shift, along the whisker axis, between the observed diffraction peaks (Plate II, fig. 1, 39) was produced by whisker orientation (Plate V, fig. 1) and twisted lattice planes resulting from an axial screw dislocation. The lattice twist, along with whisker orientation, necessary to produce the observed shift between diffraction spots is 0.048 radian per cm. This value for the lattice twist is less than the value of 0.070 radian per cm calculated from the equatorial spots of the transmission Laue pattern.

The lattice twist, necessary to produce the observed shift between diffraction peaks, of 0.048 radian per cm was calculated from a knowledge of the magnitude of the Burgers vector as determined from the tilt of the diffraction planes. The strain within the whisker, at the positions where the Burgers vector was determined, produced a compression of the lattice planes in the direction of the Burgers vector. A smaller value was thus obtained for the Burgers vector than was obtained experimentally from the Laue photograph. The value for the lattice twist 0.070 radians per cm determined from the equatorial spots of the transmission Laue diffraction pattern represents the lattice twist existing in the entire whisker. The two different values for the lattice twist are not contradictory but augment the concept that an axial

screw dislocation exists within the whisker. No correlation between the two values for the lattice twist can be made since the distribution of the strain field within the whisker is not known.

Absorption of the incident and diffracted beams within the whisker prevented the detection by intensity contrasts of the axial screw dislocation. Thus, the observed diffracted intensity maxima (Plate II, fig. 1, 2) resulted from extinction as predicted by Johnson. Using equation 8, the extinction coefficient was calculated for the two orientations of the whisker as shown in Plate IV, figures 1 and 2 and yielded $\epsilon = 0.64$ and $\epsilon = 0.46$, respectively. The average extinction coefficient is $\epsilon = 0.55 \pm 0.2$. The value of the primary extinction coefficient, ϵ_p, (equation 6), calculated by Johnson for the $(\bar{2}1\cdot0)$ diffraction planes, planes perpendicular to the growth axis, is $\epsilon_p = 19$. Whenever the extinction coefficient ϵ is within the limits $0 < \epsilon < 19$, the extinction coefficient represents secondary extinction.

Johnson, using the method and equipment similar to that used in this study, obtained an average extinction coefficient of $\epsilon = 1.2$ for the $(\bar{2}1\cdot0)$ lattice planes of a cobalt whisker having a $[10\cdot0]$ growth axis. Since the equipment and technique used in determining both values for the extinction coefficient were similar, it is assumed the difference between the two values is a result of individual crystal imperfection. Whisker Co-292 had a cross sectional dimension of 27μ x 39μ and a 72 Å Burgers vector; whereas, the whisker used by Johnson had a cross section of 10μ x 10μ and a 4.8 Å Burgers vector.

The values for the cross sectional dimension, Burgers vector, and extinction coefficient associated with each whisker tend to indicate that the imperfections producing the secondary extinction are a result of the axial screw dislocation within each whisker. If the imperfection of the crystal is

a result of the dislocation, then the different values of the extinction coefficients obtained from different regions of the diffraction planes, cannot be combined to obtain an average. The extinction coefficient determined for each region of the diffraction plane would be a measure of the dislocation effects for that region. The extinction coefficient would not represent a measure of the perfection of the crystal but would only represent the perfection for a particular region of the crystal.

EXPLANATION OF PLATE V

GEOMETRY OF WHISKER CO-292

Fig. 1. Diagram indicating possible cause of lateral shift of diffraction spots.

Fig. 2. Diagram giving measurements for calculating lateral shift of diffraction spots.

PLATE V

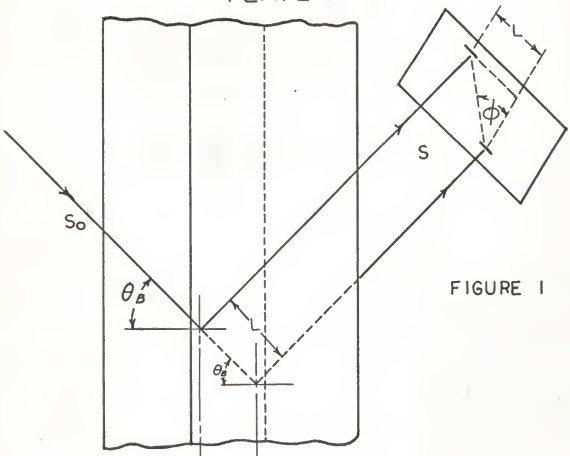

FIGURE 1

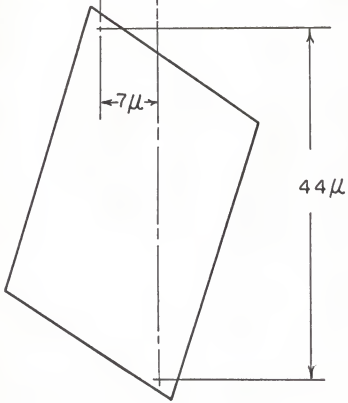

FIGURE 2

EXPLANATION OF PLATE VI

COBALT WHISKER CO-206

Fig. 1 A. Topograph showing the regions of strain when the horizontal component of the incident beam was perpendicular to one irregular side of the whisker. (x171)

B. Oscillation photograph showing the irregularity in the whisker axis. (x171)

C. Topograph obtained when the horizontal component of the incident beam was perpendicular to a regular side of the whisker and showing the location of the nuclear track plate with respect to the whisker. (x171)

D. Topograph after whisker located as in 1c had been rotated by 3 minutes of arc and showing the location of the nuclear track plate with respect to the whisker. (x171)

Fig. 2 Drawing indicating how the diffraction spots observed in fig. 1d could be obtained.

The plane of the photographic emulsion was oriented at an angle of 20° with respect to the whisker axis, see fig. 1.

PLATE VI

FIGURE 1

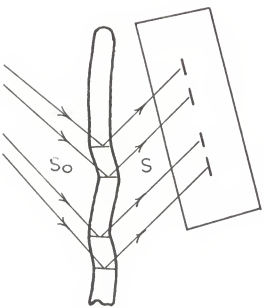

FIGURE 2

ACKNOWLEDGMENT

The author expresses sincere gratitude to Dr. R. D. Dragsdorf for his initiation of the project and his guidance through the program. Appreciation is expressed to Dr. R. Katz for use of the Leitz microscope and to R. T. Johnson and G. E. Harland for having helped build some of the equipment.

The project was sponsored by the Bureau of General Research, Kansas State University.

REFERENCES

(1) Alexander, C. A. and Smith, T. S.
Vapor pressure of cobaltous chloride. Chem. Abstracts, 52, No. 13-16, 1958, 12474a.

(2) Anantharaman, T. R.
Lattice parameters and crystallographic angles of hexagonal cobalt. Current Sci. (India), February, 1958, 27:51-53.

(3) Berg, W.
An x-ray method for study of lattice disturbances of crystals. Naturwissenschafter, 1931, 19:391-396.

(4) Barrett, C. S.
A new microscopy and its potentials. Trans. Am. Inst. Mining, Met., Petrol., Engrs. Inst. Met. Div., Tech. Pub. No. 1865, 1945, 50 p.

(5) Bönse, U.
Zur röntgenographischen bestimming des typs enzelner versetzungen in einkristallen. Z. Physik, 1958, 153:278-296.

(6) Brenner, S. S.
Growth and properties of whiskers. Science, September, 1958, 128:569-575.

(7) Brenner, S. S.
The growth of whiskers by the reduction of metal salts. Acta. Met., 1956, 4:62-74.

(8) Brenner, S. S. and Sears, G. W.
Mechanism of whisker growth. Acta. Met., 1956, 4:268-270.

(9) Dragsdorf, R. D. and Webb, W. W.
Detection of screw dislocations in α-Al_2O_3 whiskers. J. Appl. Phys., 1958, 29:817-819.

(10) Edwards, J. W., Johnson, H. C., and Ditmars, W. E.
The vapor pressures of inorganic substances. Chem. Abstracts, 46, No. 8-14, 1952, 4348i.

(11) Eshelby, J. D.
The twist in a crystal whisker containing a dislocation. Phil. Mag., 1958, 3:440-447.

(12) James, R. W.
The optical principles of the diffraction of x-rays. London: G. Bell and Sons, 1948. p. 58-60, 269-272.

(13) Johnson, R. T.
Cobalt whiskers: Their growth, dislocations, and phase change. Thesis, Kansas State University, 1957.

(14) Johnson, R. T.
A study of the effects of the cobalt transformation on the dislocation structure of cobalt whiskers using a high resolution x-ray diffraction technique. Dissertation, Kansas State University, 1963.

(15) Klyachko-Gurvich, L. L., Bulgakova, T. I., and Gerasimov, Y. I.
Interaction of cobalt oxides and sulfur oxides. Chem. Abstracts, 43, Pt 3, 1949, 6931h.

(16) Kornev, Y. V. and Golubkin, V. N.
The determination of the vapor tension and the heat of sublimination of cobalt in the 1050 to 1250° temperature range. Chem. Abstracts, 49, No. 21-23, 1955, 15320h.

(17) Schäfer, H. and Krehe, K.
Gaseous cobalt (III) chloride and its thermochemical properties. Chem. Abstracts, 46, No. 15-20, 1952, 7449g.

(18) Schäfer, H., and others.
Saturation pressures of cobaltous chloride. Chem. Abstracts, 49, No. 21-23, 1955, 15419f.

(19) Sears, G. W.
Whisker growth. Acta. Met., 1955, 3:367-369.

(20) Verma, A. R.
Crystal growth and dislocations. New York: Academic Press, 1953.

APPENDIX I

APPENDIX I

Cobalt Whisker Data

Identification Number	Growth Axis	Laue Tilt (deg)	Dimensions (μ)	Comments
206	10•0	30	7x13x200	
207	10•0			Oriented polycrystal.
225	10•0	0	12	
226	10•0	90		
227		0	5x5x1200	Unable to determine axis.
228	10•0	0	5x10x450	Lost.
230	10•0	0		
231	10•0	0		Lost.
232	10•0	15	20x15x700	Saber shape.
246	10•0	5	5x5x300	
248		0	10x10x250	Oriented polycrystal.
249			5x30x100	Ribbon.
250			5x8x250	Twisted.
251	10•1	0	400	Ribbon.
252	10•1	90	10x15x450	Oriented polycrystal.
253	10•1	0	10x10x900	
254	10•1	0	8x25x1400	
255	10•1	0	8x12x350	
256				Ribbon.
261	10•1			Oriented polycrystal.
265				Saber shape.
266			5x5x400	Twisted.
267	10•0	0		
268			5x15x400	Taper.
269				Saber shape.
270	10•0	5	8x8x800	
272	10•0		5x5x200	Oriented polycrystal.
273	10•0	10	8x8x250	
274	10•0	45		Lost.
275	10•0			Lost.
276	10•0	5	5x5x150	
277	10•0	0	5x5x325	
278	10•0	0	3x5x350	
279	10•1	0	5x8x1000	
280	10•0	0	5x8x1500	
281	10•0	0	10x20	Oriented polycrystal.
282	10•0			
283	10•0			
290	10•0	0	15x20	
291	10•0	0		Quenched.
292	10•0	15	27x39x500	
295	10•0	90		
301	10•0	0		

GROWTH, DISLOCATIONS, AND EXTINCTION OF COBALT WHISKERS

by

BILLY HUGH BAILEY

B. S., Kansas State University, 1961

AN ABSTRACT OF A THESIS

submitted in partial fulfillment of the

requirements for the degree

MASTER OF SCIENCE

Department of Physics

KANSAS STATE UNIVERSITY
Manhattan, Kansas

1964

Cobalt whiskers have been grown by deposition of metallic halide ions from a supersaturated metallic halide vapor. This technique employs an alundum boat filled with a metal halide which is placed in a hot furnace through which hydrogen is flowing. During the period of a few hours, filamentary crystals of the metal grow on the sides of the boat and on the reduced metal in the boat.

The growth procedures have been studied in order to determine some of the growth parameters. These parameters have been indicated to include the water content present during growth, the hydrogen flow rate, the metal halide grain size, and the temperature at the growth site.

The cobalt whiskers were examined using high resolution x-ray diffraction techniques in order to augment the concept that growth occurred by means of an axial screw dislocation.

If a whisker were to grow with an axial screw dislocation, there would exist a region of heavy strain surrounding the screw axis. This strain would produce an incremental change in the lattice spacing resulting in a small change in the Bragg glancing angle. The strain region would appear as a contrast in the diffracted intensity maximum.

When diffraction from a crystal occurs, the diffracted beam is partially reflected at the crystal planes and at segmented sections within the crystal. These multiple reflections result in interference between the diffracted and incident beams. Since some destructive interference will occur, there is a diminution of both the diffracted and incident beams. This effect is known as extinction and appears as an additional term to the normal absorption coefficient.

If a crystal had a linear variation in cross section and diffraction occurred from planes with normals perpendicular to this variation, the

diffracted beam should yield a point where maximum diffracted intensity occurred. By measuring the thickness of the crystal where maximum diffracted intensity occurred, an effective absorption coefficient could be determined. By measuring the effective absorption coefficient the extinction coefficient can be calculated.

In the experimental work reported in this thesis, maximum whisker growth appeared in the temperature range of 550 - 600°C. No noticeable change in growth occurred from small variations in the hydrogen flow rate.

The diffraction contrast surrounding an axial screw dislocation was not observed. Extinction and absorption produced a diffraction contrast within a diffraction maximum. The greatest contrast appeared as a decrease in the diffracted x-radiation from the lattice planes perpendicular to the whisker axis. Two distinct diffraction spots, apparent in darkest contrast and symmetric with respect to the whisker axis, were displaced from each other along the length of the whisker. This displacement was produced by the lattice twist which accompanies an axial screw dislocation. The lattice twist, calculated from the observed shift of diffraction spots, was 0.048 rad per cm as compared to the value 0.070 rad per cm which was calculated from the tilt of the equatorial spots of the transmission Laue pattern.

The extinction coefficient was calculated for two different orientations of the diffraction planes with respect to the incident beam. The average extinction coefficient for the two measurements was $\epsilon = 0.55 \pm 0.2$. A perfect cobalt crystal has an extinction coefficient of $\epsilon = 19$ and for a totally imperfect crystal $\epsilon = 0$. No relation exists relating the observed extinction coefficient to the perfection of the whisker.